Interplay between Structure and Fluidity of Model Lipid Membranes under Oxidative Attack

Wan-Yu Tai, Yi-Cyun Yang, Hui-Jen Lin, Chin-Ping Huang, Yi-Lin Cheng, Mei-Fang Chen, Hsiu-Lan Yen, and Ian Liau*

Department of Applied Chemistry and Institute of Molecular Science, National Chiao Tung University, Hsinchu 300, Taiwan

A proper regulation of membrane fluidity is critical for cellular activities such as communication between cells, mitosis, and endocytosis. Unsaturated lipids, a main component of biological membranes, are particularly susceptible to oxidative attack of reactive oxygen species. The oxidation of lipids can produce structural derangement of membranes and eventually alter the membrane fluidity. We have applied fluorescence correlation spectroscopy (FCS) and Raman spectroscopy to investigate the fluidity and structure of model membranes subject to oxidative attack. Hydrogen peroxide has little effect on the lateral fluidity of membranes, whereas hydroxyl radical causes a significantly increased fluidity. The latter is rationalized with the cleavage of the acyl chains of lipids caused by hydroxyl radical; this interpretation is founded on the diminished intensities of lines in Raman spectra associated with $-CH_2$ and $C=C$ moieties in lipids and supported by mass-spectral measurements. The same approach provides a mechanistic account of the inhibitory capability of vitamins C and E against the increased membrane fluidity resulting from an oxidative attack. Membranes with much cholesterol exhibit a novel resistance against altered membrane fluidity induced with oxidative attack; this finding has biological implications. Our approach combining FCS and Raman measurements reveals the interplay between the structure and fluidity of membranes and provides insight into the pathophysiology of cellular oxidative injury.

Introduction

The regulation of membrane fluidity, especially the lateral diffusion of molecules on biological membranes, is essential for cells to maintain vital activities such as cell motility, mitosis, recognition, endocytosis, and phagocytosis.[1–10] An altered membrane fluidity has been observed to occur concurrently with, or has been implicated in, various diseases.[11–16]

The fluidity of biological membranes is controlled mainly by their compositions.[17,18] Membranes made of lipids with short acyl chains, or with many unsaturated $C=C$ moieties in the fatty chain, tend to have great fluidity.[19] As a result, an external stress that causes structural modification of the constituent lipids of membranes would yield also an altered membrane fluidity. Through their reactivity, unsaturated lipids, a main component of biological membranes, are susceptible to the oxidative attack of endogenous reactive oxygen species (ROS), such as hydrogen peroxide (H_2O_2) and hydroxyl radical ($OH^•$).[20,21] Despite considerable effort to observe the modification of membrane fluidity induced by oxidative attack, few provide mechanistic or structural account to this alteration. Among contradictory conclusions reported, increased fluidity was observed for brain synaptic plasma membranes[12] and hepatocyte membranes[16] under oxidative attack, whereas lipid peroxidation was associated with decreased fluidity on erythrocyte membranes.[13,15] This inconsistency emphasizes the necessity to characterize systematically the interplay between structure and fluidity of membranes under oxidative attack.

The search for effective therapies to inhibit cellular oxidative injury has increased markedly in view of the implication of oxidative injury in many diseases. L-ascorbic acid (vitamin C) and α-tocopherol (vitamin E) are generally regarded as protecting lipid membranes from the injurious effect of ROS,[22,23] but specific questions, such as whether both vitamins employ the same protective mechanism, remain largely unanswered. Vitamin C acts as a scavenger of ROS through antioxidation, whereas vitamin E bound to membranes acts as a stabilizer to maintain the integrity of membranes beyond its function as an antioxidant.[24,25] Elucidation of the mechanism that underlies the inhibition of altered membrane fluidity is important for the development of effective therapies against cellular oxidative injury.

Being principal constituent of the membranes of both mammalian cells and intracellular organelles, cholesterol has maintained intense interest.[26–28] It not only regulates the bulk physical properties of membranes, but also engages in specific interaction with other membrane constituents such as proteins. The cholesterol content of membranes varies significantly among cell types or organelles;[29,30] for example, the plasma membrane of human erythrocytes contains approximately 45 mol % cholesterol with respect to other membrane lipids, whereas the membrane of intracellular organelles such as mitochondria and endoplasmic reticulum contains less than 10 mol %.[31] Although the modulation of membrane fluidity by cholesterol has been investigated,[18,19] whether cholesterol specifically affects the ROS-induced alteration of membrane fluidity has barely been addressed. In view of the large variation of cholesterol content among cells or organelles, an answer to the above question should provide clues to the fates of various cells or organelles under oxidative attack.

---

* To whom correspondence should be addressed. E-mail: ianliau@mail.nctu.edu.tw.

Model Lipid Membranes under Oxidative Attack

J. Phys. Chem. B, Vol. 114, No. 47, 2010 **15643**

To investigate the interplay between the structure and the fluidity of membranes under oxidative attack, we employed a parallel approach based on fluorescence correlation spectroscopy (FCS),[32−35] to characterize the lateral diffusion of molecules on membranes, and Raman spectroscopy,[36−38] to characterize the structure of lipid molecules of single optically trapped liposomes. We compared the alteration of membrane fluidity under treatment with two ROS, hydrogen peroxide and hydroxyl radical, and examined the ability of vitamins C and E to inhibit this change. We show that Raman spectra provide structural information to account for the fluidity change. In our investigation of membranes comprising varied cholesterol content, we discovered a novel inhibitory effect of membrane-bound cholesterol against ROS-induced alteration of membrane fluidity. The results are rationalized with complementary Raman spectra. Our result demonstrates the unique capability of this parallel approach and indicates its potential to enhance our understanding of cellular oxidative injury.

Materials and Methods

Reagents. 1,2-Dioleoyl-sn-glycero-3-phosphocholine (DOPC, Avanti Polar Lipids), 1,1′-dioctadecyl-3,3,3′,3′-tetramethylindodicarbocyanine perchlorate (DiD), 3,3′-dioctadecyloxacarbocyanine perchlorate (DiO) and Alexa Flour 633 (Invitrogen), trichloromethane and menthol (J.T. Baker), cholesterol, glucose, sodium chloride (NaCl), hydrogen peroxide, $FeSO_4 \cdot 7H_2O$, L-ascorbic acid and α-tocopherol (Sigma Aldrich) were obtained from the indicated sources.

Hydroxyl radical was prepared on mixing equal amounts of solutions of H_2O_2 and $FeSO_4$; its concentration was estimated assuming the reaction between Fe^{2+} and H_2O_2 to proceed to completion.[38]

Vitamin C solution was prepared on dissolving L-ascorbic acid in deionized water and was mixed with a solution containing lipid vesicles prior to measurements.

Preparation of Giant Unilaminar Vesicles (GUV). We employed electroformation to prepare GUV according to a reported protocol.[39] In brief, we prepared an appropriate mixture of lipid and cholesterol in a solution containing trichloromethane and methanol (volume ratio 9:1), transferred the solution (20 μL) to a glass slide coated with indium tin oxide (ITO), and kept the slide under vacuum for at least 1 h to evaporate the solvent. We then placed a silicone spacer on the slide, added a solution of glucose (600 μL, 0.2 M) to the slide, and sealed the solution with another ITO-coated glass slide. To produce vesicles, we supplied an alternating bias (sinusoidal waveform, $V_{pp} = 3$ V, $f = 10$ Hz) to the two conducting slides for 3 h. All subsequent measurements were performed at 22 ± 1 °C. To prepare GUV containing vitamin E, the same protocol used to prepare DOPC GUV was followed except that a small amount of vitamin E was mixed with DOPC (molar ratio 1:20) in the solution.

For confocal fluorescence imaging and FCS measurements, we used two fluorescent probes specific to lipids, DiO and DiD, respectively, to label vesicles. The preparation of the fluorescence-labeled vesicles was identical to that of nonlabeled vesicles, except that the labeling agents (molar ratios 10^{-3} for confocal fluorescence imaging and 10^{-5} for FCS measurements) were mixed in a small portion with lipids in the solution. The diameter of vesicles prepared in this way ranged mostly between 20 and 30 μm, as can be seen from the confocal images displayed in Figure 1.

FCS Measurements. A schematic of our constructed FCS system used in this work is shown in Figure 2A. The beam of
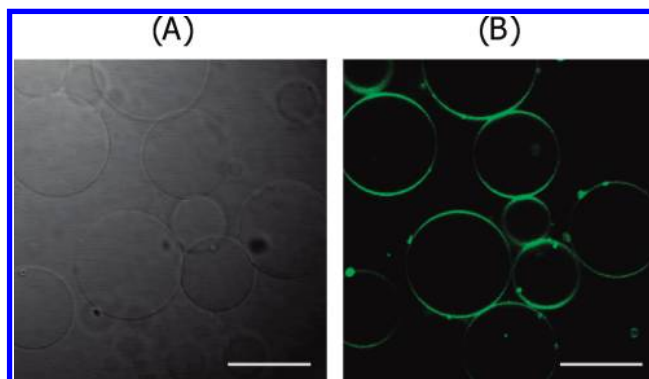

Figure 1. Microscopic images of fluorescence-labeled vesicles. (A) Phase-contrast and (B) confocal fluorescence images. The fluorescence-labeled giant unilaminar vesicles were prepared on mixing DOPC lipids and fluorescent lipid analogues, DiO molecules, at a molar ratio 1000:1. Scale bar: 20 μm.

the HeNe laser (1137P, JDS Uniphase, U.S.A.) for excitation was expanded and collimated to a diameter about 1 cm with a spatial filter. The collimated beam was directed to an inverted optical microscope (IX 71, Olympus, Japan) through the back-port using a dichroic mirror and was focused onto the sample with a microscope objective (60× PlanApo, water immersion, numerical aperture 1.2, Olympus, Japan). The typical laser power illuminating the sample was 38 μW. A three-axis piezo stage (PI-563CD, Physik Instrumente, Germany) integrated into the sample stage of the microscope served to position the vesicles with respect to the laser focus. The emitted fluorescence was collected in an epi direction, passed through the dichroic mirror and a bandpass filter, and detected with a fiber-coupled avalanche photodiode (APD, SPCM-AQR-15-FC; PerkinElmer Optoelectronic, Canada). The optical fiber (core diameter 50 μm) acted as a pinhole to achieve confocal detection. The autocorrelation function of the fluctuating fluorescence signal was calculated in real time with a hardware correlator (Correlator.com, U.S.A).

To derive the diffusion coefficient of DiD molecules on membranes, we fitted the autocorrelation function with an equation based on a model of two-dimensional diffusion[34,40,41]

$$G(\tau) = \frac{1}{N}\left[1 + \frac{\tau}{\tau_D}\right]^{-1}$$

in which $G(\tau)$ is the autocorrelation function, N is the effective number of DiD molecules within the detection zone, τ is the delay time and τ_D is the diffusion time. Data fitting was performed with an algorithm based on least-squares. After the diffusion time was obtained from the best fit, the diffusion coefficient, D, was calculated from

$$D = \frac{r_0^2}{4\tau_D}$$

in which r_0, the waist ($1/e^2$ radius) of the focal zone, is a system parameter that was determined independently using a reference molecule of known diffusion coefficient in solution. Figure 2B shows an autocorrelation curve obtained from a reference (Alexa 633) in solution. Using a diffusion coefficient $D = 1.35 \times 10^{-10}$ m^2 s^{-1}, we determined the waist of the focal zone to be 203 nm. For comparison, a representative autocorrelation curve measured from DiD molecules on membranes is included.
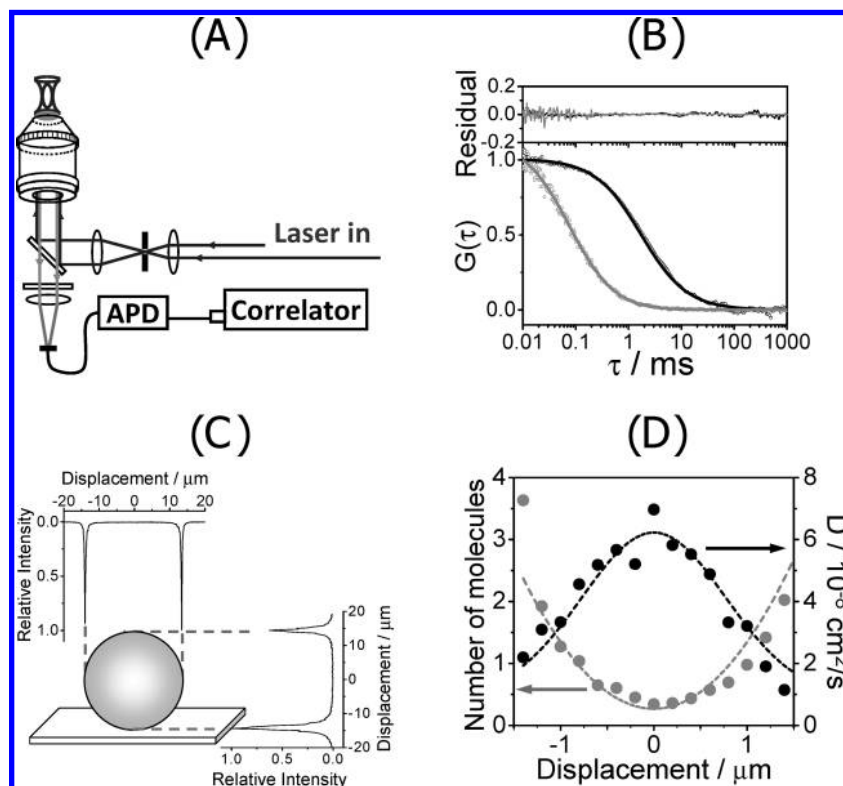
Figure 2. Setup of fluorescence correlation spectroscopy. (A) Schematic of the apparatus for FCS measurements. (B) Representative autocorrelation functions measured on R6G molecules in solution (gray circles), and on DiD molecules on a DOPC membrane (black circles). The autocorrelation function of R6G molecules in solution was fitted with a model of three-dimensional diffusion (gray line), whereas that of DiD molecules on membranes with a model of two-dimensional diffusion (black line). The residual showing the minor difference between the raw data and the best fit are displayed in the upper panel. (C) Cross-section views of a single giant unilaminar vesicle displayed as line-scan intensity in lateral and vertical directions. (D) Diffusion coefficient (black) and the effective number of molecules (gray) at varied depths near the upper surface of the vesicle.

We measured only vesicles of similar size (diameter ~25 μm). The large size relative to the dimension of the detection zone ensured that the curvature of the membrane had a negligible effect. For consistency, all FCS measurements were performed near the center of the upper membrane of vesicles. We first located the center of an arbitrary focal plan within a vesicle and then translated the vesicle in the vertical direction to obtain a maximal intensity of fluorescence. Representative cross-section intensities of lateral and vertical scans are shown in Figure 2C. We estimated that the lateral and vertical resolutions of our apparatus were 0.3 and 1.1 μm, respectively, from the full width at half-maximum of these line scans. To improve the alignment of the laser focus with the upper membrane, we measured depth-resolved FCS with step size 0.2 μm. Figure 2D shows the diffusion coefficient and the effective number of molecules at varied depths near the upper surface of a vesicle. Subsequent FCS measurements were made at the depth that yielded the largest diffusion coefficient and the smallest number of fluorescent molecules. Typically, 10 successive measurements (duration 10 s) were performed for each vesicle to obtain a statistical mean.

Raman Spectral Measurements on Single Liposomes. We employed "Raman tweezers" to measure temporally varying Raman spectra of single optically trapped liposomes and to characterize kinetically the structural modification of lipid molecules under treatment with ROS; details of this apparatus are reported elsewhere.[38] In brief, a diode-pumped solid-state laser (532 nm, DPSS Inc., U.S.A.) served both to capture a single lipid liposome and to generate Raman scattering from the optically trapped liposome. The backscattered Raman signal was recorded with a spectrometer (SpectraPro 2300, Princeton

Instruments, U.S.A.). We continuously recorded the spectra of a single liposome for as long as 60 min with an acquisition duration 60 s for each spectrum. From each spectrum we subtracted the background; the serial changes of each line were expressed as the fold of change relative to the baseline spectrum obtained in the first minute. The spectral resolution of the system, 1.6 cm^{-1}, was determined from the full width at half-maximum of the line of polystyrene at 1001 cm^{-1}.

Statistical Methods. Comparison between the means of two groups was made using the two-tailed Student's t test. The levels of statistical significance were set at $P < 0.05$, $P < 0.01$, and $P < 0.001$, respectively.

Results and Discussion

Oxidative Attack Causes an Increase of Membrane Fluidity through Cleavage of the Acyl Chain of Lipids. We sought first to determine how a treatment with ROS altered the membrane fluidity. Figure 3A displays representative autocorrelation curves of DiD molecules on DOPC membranes obtained before and after exposure (60 min) to hydroxyl radical (0.05 mM); results obtained under treatment with hydrogen peroxide (0.05 mM) are shown in Figure 3B. A comparison of these results shows that the treatment with hydroxyl radical caused the autocorrelation curve to shift to the left, whereas treatment with hydrogen peroxide yielded no discernible alteration of the autocorrelation curve.

The diffusion coefficients of DiD molecules obtained on membranes subject to the two treatments are shown in Figure 3C; the diffusion coefficient increased by 62% (6.52×10^{-8} vs 10.59×10^{-8} cm^2 s^{-1}, $P = 5.87 \times 10^{-8}$) when the membrane

Model Lipid Membranes under Oxidative Attack

J. Phys. Chem. B, Vol. 114, No. 47, 2010 **15645**
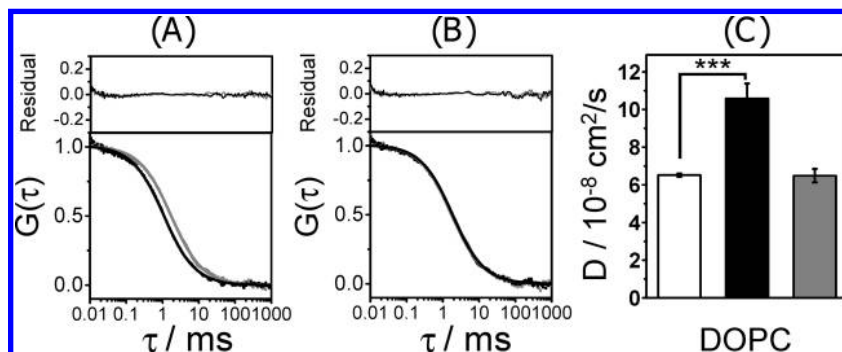

Figure 3. Change of membrane fluidity before and after oxidative attack. (A) Autocorrelation function measured before (gray) and after (black) a treatment with hydroxyl radical (0.05 mM); raw data (circles), best fit (line), and residual (upper panel). (B) Result obtained on treatment with hydrogen peroxide (0.05 mM). (C) Comparison of diffusion coefficients of DiD molecules measured on membranes under varied treatments (normal control, empty bar $n = 29$; treatment with hydroxyl radical, solid black bar $n = 31$; treatment with hydrogen peroxide, gray bar $n = 12$; ***$P < 0.001$, **$P < 0.01$, *$P < 0.05$, NS $P > 0.05$, insignificant).
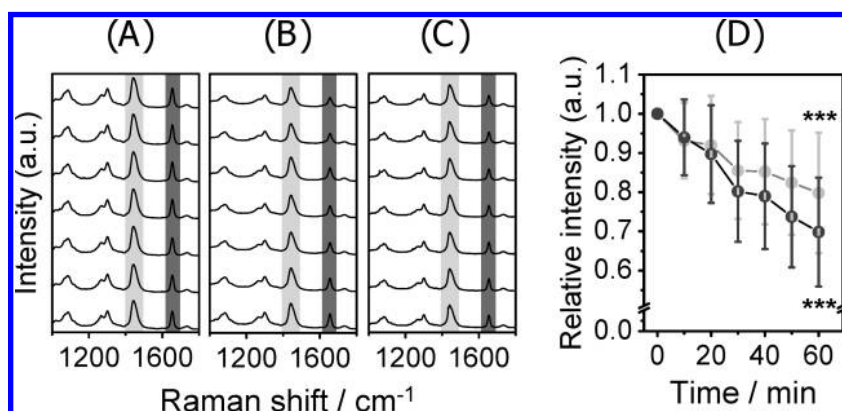

Figure 4. Change of Raman spectra before and after oxidative attack. (A−C) Temporally varying Raman spectra of a single liposome under varied treatments: normal control (A), hydroxyl radical (0.05 mM) (B), and hydrogen peroxide (0.05 mM) (C). The spectra were recorded in a sequence each 10 min with the first spectrum ($t = 0$) displayed at the bottom. To facilitate comparison of these spectra, Raman lines at 1440 and 1650 cm^{-1} have been highlighted in light and dark gray, respectively. (D) Temporal evolution of the two Raman lines measured on single liposomes treated with hydroxyl radical. (light gray, 1440 cm^{-1} $n = 10$; dark gray, 1650 cm^{-1} $n = 10$; ***$P < 0.001$, **$P < 0.01$, *$P < 0.05$, NS $P > 0.05$, insignificant).

was treated with hydroxyl radical for 60 min, whereas the change was insignificant with the treatment of hydrogen peroxide (6.52×10^{-8} vs 6.49×10^{-8} cm^2 s^{-1}, $P = 0.88$). This finding clearly shows that the exposure of the membranes to hydroxyl radical produced a greatly increased membrane fluidity, whereas hydrogen peroxide, if not converted to hydroxyl radical, had little effect on the membrane fluidity.

To provide a structural account of the ROS-induced alteration of membrane fluidity, we employed kinetic Raman measurements to characterize the spectral variation of liposomes comprising DOPC lipids under treatment with hydroxyl radical or hydrogen peroxide; the results are displayed in Figure 4. To facilitate a comparison of the progressive spectral changes, we highlighted the two most pronounced Raman lines, at 1440 cm^{-1} attributed to the CH$_2$-bending mode (light gray) and at 1650 cm^{-1} attributed to the C=C-stretching mode (dark gray). As seen from Figure 4A, the sequential Raman spectra of the control (i.e., with no treatment) exhibited no appreciable temporal variation (>60 min) confirming that a prolonged exposure of DOPC liposomes to laser illumination incurred no discernible damage under our experimental condition. When the liposome was treated with hydroxyl radical (0.05 mM), both specified Raman lines diminished progressively (Figure 4B). In contrast, the sequential Raman spectra of a single liposome on treatment with hydrogen peroxide (0.05 mM) remained essentially constant (Figure 4C).

The decreased intensity of the Raman line at 1650 cm^{-1} (C=C stretching mode) offers a sensitive means to probe the

progression of lipid peroxidation in both biological cells and liposomes comprising monounsaturated lipids.[38,42] The present work confirms that conclusion by showing that a treatment with hydroxyl radical induced peroxidation of DOPC lipids. It also shows that, in contrast to hydroxyl radical, hydrogen peroxide is insufficiently reactive to cause discernible structural modification.

Figures 4 and 3 clearly show that the variation of the Raman spectra exhibited a trend consistent with that of the diffusion coefficients according to the results of treatments with hydroxyl radical and hydrogen peroxide. As Raman spectra provide structural information, this observation indicates a strong correlation between the alteration of the membrane fluidity and the modification of the lipid structures. We sought to account for the observed increase of membrane fluidity by solving the structural clues of Raman spectra. We analyzed the sequential variation of the Raman spectra of single optically trapped liposomes subject to the treatment with hydroxyl radical ($n = 10$); the temporally varying intensities of the Raman lines at 1440 and 1650 cm^{-1} are displayed in Figure 4D. After exposure (60 min) to hydroxyl radical, the intensities of both Raman lines decreased, by 20% (light gray, $P = 8.39 \times 10^{-4}$) and 30% (dark gray, $P = 1.17 \times 10^{-5}$), respectively. As the intensities of the two specified Raman lines are proportional to the number of CH$_2$ and C=C moieties, and as the Raman tweezers measured only molecules that remained on the optically trapped liposomes rather than being dissolved in solution, the decreased Raman intensities strongly indicate the cleavage of the acyl chain of lipids caused by the oxidative attack of hydroxyl radical.
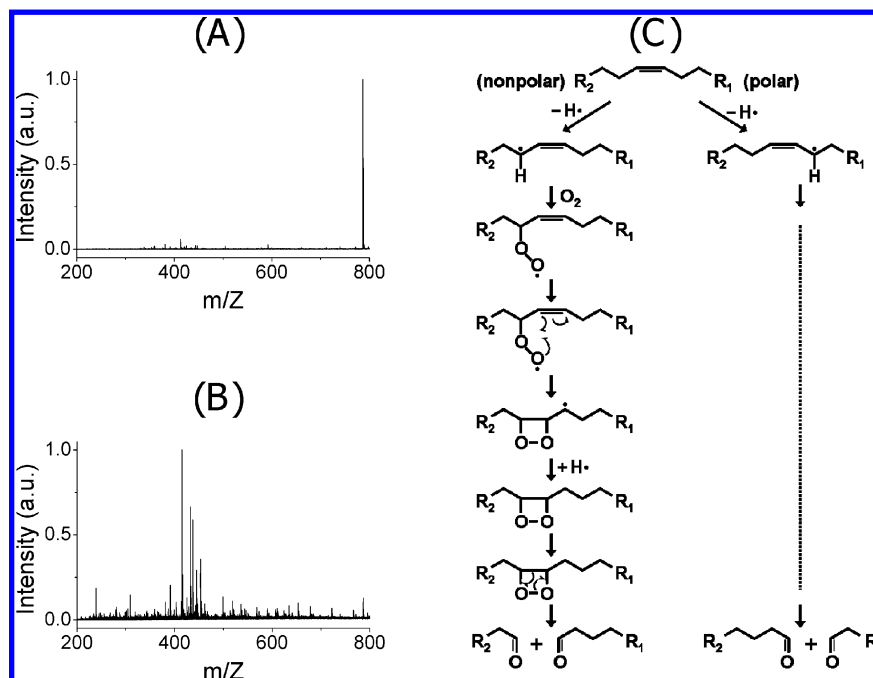
Figure 5. Mass spectra and a proposed mechanism to account for the cleavage of lipids caused by treatment with hydroxyl radical. (A) Mass spectrum of lipids without treatment. (B) Mass spectrum of lipids measured after treatment of hydroxyl radical. (C) A proposed mechanism illustrating the cleavage of lipids caused by the attack of hydroxyl radical and the generation of fragments with decreased chain lengths.

To consolidate these deductions, we compared the mass spectra of lipids with and without treatment with hydroxyl radical. The mass spectrum of the control (without treatment) possessed only a single line corresponding to the molecular ion of the DOPC lipid (ratio of mass to charge, $m/z = 785.93$ u, Figure 5A), whereas that of the treated sample exhibited numerous lines corresponding to ions with masses smaller than that of the parent ion (Figure 5B). These results provide compelling evidence to confirm the deduction from the Raman measurements; that is, the treatment of DOPC with hydroxyl radical caused cleavage of the acyl chain of lipids.

The observation of numerous lines in Figure 5B indicates that complicated reactions were involved and diverse products arose from the treatment of lipids with hydroxyl radical. This result is expected because hydroxyl radical is highly reactive and can produce varied radicals that complicated chain reactions. We propose further a mechanism to account qualitatively for the observation of numerous lines in mass spectra. As illustrated in Figure 5C, the reaction might begin with the abstraction of an allylic hydrogen from the unsaturated lipid by hydroxyl radical. The resulting allylic radical can then couple with molecular oxygen (O_2), yielding a peroxyl radical.[43] The peroxide radical might then undergo cyclization[44] and abstract a hydrogen atom from neighboring lipids, yielding a 1,2-dioxetane. Lastly, the decomposition of the unstable 1,2-dioxetane would lead to generation of two carbonyl fragments resulting in the cleavage of the lipid.[45]

The distal end of the two fragments (i.e., the one that contains the nonpolar end of the lipid) is essentially an aldehyde and would dissolve in the solution. In contrast, the other fragment that contains the polar head of the lipid would remain part of the membrane, but become shorter than other lipid molecules that have not undergone the same reaction. The cleavage of the lipid and the dissolution of the aldehyde are consistent with the diminished Raman intensities shown in Figure 4B,D. As the reaction proceeds, the membrane would comprise more lipid molecules with sliced and thus shorter acyl chains. These lipids possess mismatched lengths relative to the other lipids and would

perturb the integrity of the membrane,[3] thereby producing the observed increase of membrane fluidity shown in Figure 3A,C.

In sum, our Raman spectral measurements indicate the cleavage of lipids as the membrane was treated with hydroxyl radical and provide a structural basis of the increased fluidity for membranes under oxidative attack. The interpretation is supported with the complementary mass spectra and rationalized with a plausible mechanism. In comparison with previous work of which only the alteration of membrane fluidity was reported but little direct structural evidence of the observed change was provided,[12,16,46] our work demonstrates that a parallel approach with Raman and FCS measurements can reveal the delicate interplay between structure and fluidity for membranes under oxidative attack.

Vitamins C and E Inhibit Alteration of Membrane Fluidity Induced by Lipid Peroxidation. We applied the same approach to elucidate the underlying inhibitory effects of vitamins C and E against the altered membrane fluidity induced by oxidative attack. We first measured the diffusion coefficients of DiD molecules on DOPC membranes treated with vitamin C only (1 mM, the control), or cotreated with vitamin C (1 mM) and hydroxyl radical (0.05 mM). The results, displayed in Figure 6A, show that the two diffusion coefficients varied insignificantly ($D = 5.80 \times 10^{-8}$ cm^2 s^{-1} vs 6.08×10^{-8} cm^2 s^{-1}, $P = 0.494$) in contrast to the result shown in Figure 3C for which the treatment with hydroxyl radical caused a significant increase in membrane fluidity. Co-treatment of vitamin C has effectively inhibited the change of membrane fluidity induced with hydroxyl radical.

Following the same approach, we examined the Raman spectra of single liposomes. As shown in Figure 6B, the temporally variation of Raman intensity at 1650 cm^{-1} (C=C stretching mode) remains virtually constant ($P = 0.43962$). This invariant Raman line shows unambiguously that vitamin C effectively prevented the oxidation of unsaturated lipids. This observation is consistent with the corresponding result of membrane fluidity (Figure 6A) thereby confirming that anti-oxidation is the underlying mechanism for vitamin C to inhibit
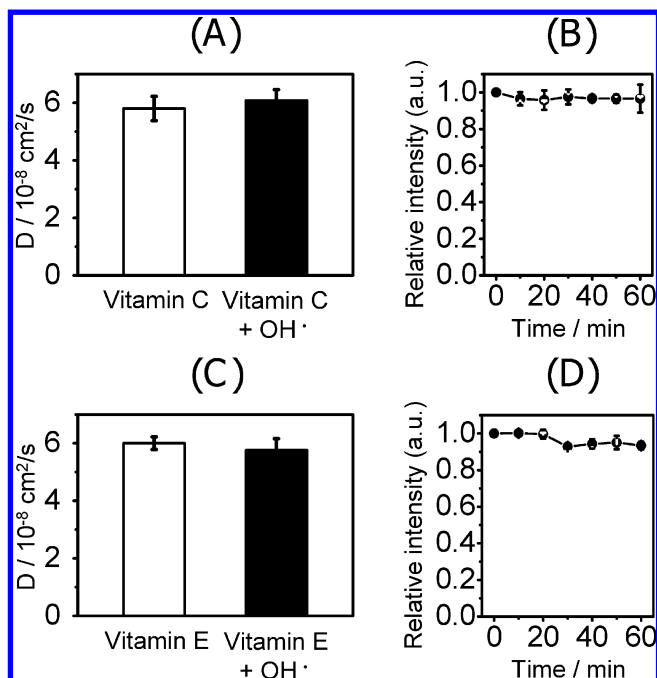
Model Lipid Membranes under Oxidative Attack

J. Phys. Chem. B, Vol. 114, No. 47, 2010 **15647**

Figure 6. Effect of antioxidants on the fluidity and Raman spectra of vesicles under oxidative attack. (A) Comparison of diffusion coefficients of DiD molecules on DOPC membranes treated with vitamin C only (empty bar), or cotreated with vitamin C and hydroxyl radical (solid black bar). (B) Temporal evolution of the Raman line at 1650 cm^{-1} (gray, liposome treated with vitamin C only $n = 5$; black, liposome cotreated with vitamin C and hydroxyl radical $n = 4$). (C) Comparison of diffusion coefficients of DiD molecules on DOPC membranes incorporating vitamin E before (empty bar) and after (solid black bar) treatment with hydroxyl radical. (D) Temporal evolution of the Raman line at 1650 cm^{-1} measured on a liposome incorporating vitamin E (gray, control $n = 9$; black, treated with hydroxyl radical $n = 4$). ***$P < 0.001$, **$P < 0.01$, *$P < 0.05$, NS $P > 0.05$, insignificant.

the increased membrane fluidity induced by hydroxyl radical. Although this conclusion is conventional wisdom,[47,48] this result demonstrates that correlated Raman and FCS measurements provide a structural account of the modification of membrane fluidity under oxidative attack.

The result of corresponding measurements on DOPC membranes incorporating vitamin E is displayed in Figure 6C, which shows that vitamin E exhibited a similar capability in maintaining the fluidity of membranes under attack from hydroxyl radical ($D = 6.00 \times 10^{-8}$ vs 5.76×10^{-8} cm^2 s^{-1}, $P = 0.081$). We then employed Raman spectral measurements to determine whether antioxidation or membrane stabilization is responsible for the unchanged membrane fluidity. According to the data shown in Figure 6D, the intensity of the Raman line at 1650 cm^{-1} of liposomes incorporating vitamin E remained unaltered in the presence of hydroxyl radical. This result clearly shows that vitamin E bound to the membrane effectively inhibited the oxidation of lipids and accounts satisfactorily for the observed intact membrane fluidity.[48] Despite our result not excluding a contribution from increased stability due to the incorporation of vitamin E, the result indicates that this mechanism might not be essential to maintain fluidity for membranes under the attack of oxidative reagents.

Effect of Cholesterol on the Altered Membrane Fluidity Induced by Oxidative Attack. We measured the fluidity of membranes comprising a binary mixture of lipid and cholesterol with varied ratios. Figure 7 shows the diffusion coefficients of DiD molecules plotted as a function of the molar ratio of cholesterol in total lipids, whereas the inset shows the autocor-
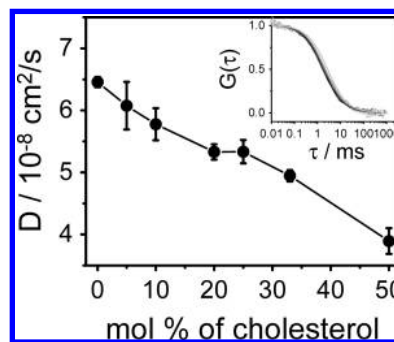

Figure 7. Effect of the cholesterol ratio on the membrane fluidity. Diffusion coefficients of DiD molecules measured on membranes with varied ratio of cholesterol. Inset: representative autocorrelation curves obtained on membranes comprising four selected fractions of cholesterol (molar ratio: 0, 10, 25, and 50%).

relation curves used to derive these diffusion coefficients. For clarity, only four curves (molar ratios of cholesterol in total lipids 0, 10, 25, and 50%) are displayed. The membrane fluidity clearly exhibits a gradual decrease with increasing content of cholesterol, except that the trend seems to become saturated in the range between 20 and 25%. The behavior resembling a phase transition indicates an onset of the formation of cholesterol-rich domains on membranes. A similar trend has been observed for membranes comprising cholesterol and various lipids; our observation agrees both qualitatively and quantitatively with the reported result.[19]

We examined whether the cholesterol ratio in lipid membranes affects the change of membrane fluidity due to oxidative attack. A comparison of the diffusion coefficients measured before (white) and after (black) treatment with hydroxyl radical for membranes comprising varied cholesterol ratios (molar ratios of cholesterol in total lipids 0, 10, 25, and 50%) is shown in Figure 8A. The increase in membrane fluidity that was caused by oxidative attack showed a strong dependence on the ratio of cholesterol in lipid membranes. The fluidity of membranes that comprised little cholesterol (such as 0 and 10%) exhibited a great increase after exposure (60 min) to hydroxyl radical, whereas the fluidity increased to a smaller extent under the same treatment for membranes containing more cholesterol (62% increase for a membrane with 0% of cholesterol, $P = 5.87 \times 10^{-8}$; 34% increase for a membrane with 10% of cholesterol, $P = 2.91 \times 10^{-7}$; 14% increase for a membrane with 25% of cholesterol, $P = 0.0281$). Most significantly, the treatment with hydroxyl radical showed no discernible effect on the fluidity when the cholesterol ratio of membranes was increased to 50% (3.88×10^{-8} cm^2 s^{-1} vs 3.99×10^{-8} cm^2 s^{-1}, $P = 0.461609$). The incorporation of cholesterol into lipid membranes partially inhibited (10 and 25% of cholesterol), or entirely prevent (50% of cholesterol), an increased fluidity of a membrane caused by the oxidative attack from hydroxyl radical.

This novel inhibitory effect of cholesterol to the increased membrane fluidity caused specifically by the oxidative attack has never been reported. To elucidate the underlying mechanism and to demonstrate further the capability of the combined FCS and Raman approach, we measured Raman spectra of liposomes comprising cholesterol of varied content under treatment with hydroxyl radical and the result is shown in Figure 8B. Similar to the result obtained on liposomes made of pure DOPC, the temporally variation of Raman intensity at 1650 cm^{-1} (C=C stretching mode) exhibited a gradual decrease for liposomes comprising both DOPC and cholesterol. Comparison of the results displayed in Figure 8B further shows that the extent of
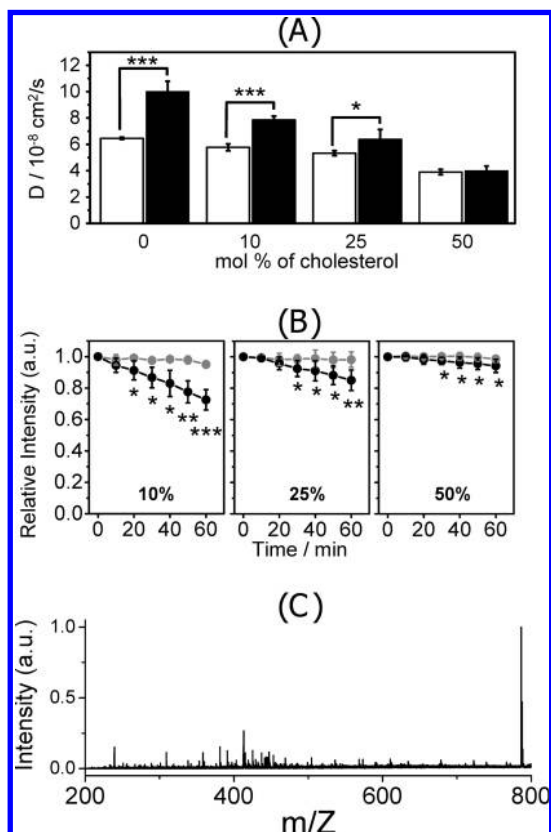
Figure 8. Change of membranes induced by oxidative attack with varied cholesterol ratios. (A) Diffusion coefficients measured before (empty bar) and after (solid black bar) treatment with hydroxyl radical for membranes with varied molar ratios of cholesterol in total lipids. (B) Temporal variation of intensity of the Raman line at 1650 cm^{-1} of single liposomes comprising varied content of cholesterol under the same treatment (gray, control; black, treated with hydroxyl radical). ***$P < 0.001$, **$P < 0.01$, *$P < 0.05$, NS $P > 0.05$, insignificant. (C) Mass spectrum of liposomes comprising 50% of cholesterol measured after the treatment of hydroxyl radical.

the decrease in the Raman intensity was significantly reduced with increasing content of cholesterol. This observation suggests that cholesterol exhibited an antioxidation capability to decrease the extent of lipid peroxidation, an interpretation that also accounts for the inhibition of the increased membrane fluidity that was caused by the attack of hydroxyl radical (Figure 8A).

To support this deduction, we carried out mass spectral measurements on liposomes comprising 50% of cholesterol after the treatment of hydroxyl radical, and the result is displayed in Figure 8C. As clearly seen from the mass spectrum, the line corresponding to the parent ion of DOPC remains largely intact, and the fragmentation caused by hydroxyl radical is largely suppressed, unlike the result obtained on pure DOPC liposome showing numerous fragments and a largely diminished line corresponding to the parent ion of DOPC (Figure 5B). This result unambiguously shows that cholesterol can inhibit lipid peroxidation and corroborates our deduction based on the results of Raman measurements. Taken together, these results once again demonstrate the ability of combined Raman and FCS measurements to reveal the interplay between structure and fluidity of membranes under oxidative attack.

Comparison of the results displayed in Figure 8A,B also shows that the mechanism of antioxidation cannot alone account entirely for the result obtained for membranes containing 50% cholesterol; the membrane fluidity remained unaltered while the intensity of the line at 1650 cm^{-1} slightly decreased. As the

membrane fluidity decreased greatly when the fraction of cholesterol exceeded 30%, and as we have related the decreased fluidity to a phase transition, the above finding can be attributed at least in part to the onset of a phase transition that might accompany the formation of microdomains rich in cholesterol.[49] We conclude that in addition to the capacity of antioxidation the formation of microdomains or a phase transition occurring in membranes with much cholesterol might also play roles in preventing membranes from a greatly increased fluidity under the attack from hydroxyl radical.

This strong dependence of the alteration of membrane fluidity induced by oxidation on the cholesterol content indicates that the cholesterol content of biological membranes (in cells and intracellular organelles) might have a pronounced effect on the ultimate fate of membranes under attack from oxidizing agents, as far as membrane fluidity is concerned. According to our results, membranes with small cholesterol content tend to have a significantly increased fluidity under oxidative attack. The percentage of cholesterol in the total lipids of mitochondrial membranes is only 10%,[7] and the mitochondrion is particularly prone to oxidative attack due to its proximity to the site of ROS production.[50,51] Our results suggests that the mitochondrion is not only vulnerable to oxidative attack but also susceptible to greatly altered membrane fluidity. As many vital mitochondrial activities are facilitated by enzymes bound to its membrane, drastic alteration of membrane fluidity would presumably compromise these functions. In contrast, lipid membranes comprising more cholesterol (such as myelin sheath[27]) might possess a resistance to the change of membrane fluidity, and survive under oxidative attack.

Conclusions

Using FCS and Raman measurements, we have characterized the lateral fluidity of membranes and the structure of lipids in model membranes under oxidative attack. Hydroxyl radical caused a significantly increased membrane fluidity. We demonstrated the ability of vitamins C and E to inhibit this ROS-induced alteration of membrane fluidity. All these results are explained according to the structural modification of lipids deduced from Raman spectra. We identified a novel resistance of membranes with much cholesterol against ROS-induced alteration of membrane fluidity and discussed its implication to cellular oxidative injury. Our results demonstrate the unique capability of the parallel approach based on FCS and Raman measurements to reveal an interplay between the structure and fluidity of membranes.

References and Notes

(1) Vereb, G.; Szollosi, J.; Matko, J.; Nagy, P.; Farkas, T.; Vigh, L.; Matyus, L.; Waldmann, T. A.; Damjanovich, S. *Proc. Natl. Acad. Sci. U.S.A.* **2003**, *100*, 8053–8058.

(2) Pande, A. H.; Qin, S.; Tatulian, S. A. *Biophys. J.* **2005**, *88*, 4084–4094.

(3) Seu, K. J.; Cambrea, L. R.; Everly, R. M.; Hovis, J. S. *Biophys. J.* **2006**, *91*, 3727–3735.

(4) Marguet, D.; Lenne, P. F.; Rigneault, H.; He, H. T. *EMBO J.* **2006**, *25*, 3446–3457.

Model Lipid Membranes under Oxidative Attack

J. Phys. Chem. B, Vol. 114, No. 47, 2010 **15649**

(5) Nishimura, S. Y.; Vrljic, M.; Klein, L. O.; McConnell, H. M.; Moerner, W. E. *Biophys. J.* **2006**, *90*, 927–938.

(6) Golebiewska, U.; Nyako, M.; Woturski, W.; Zaitseva, I.; McLaughlin, S. *Mol. Biol. Cell* **2008**, *19*, 1663–1669.

(7) van Meer, G.; Voelker, D. R.; Feigenson, G. W. *Nat. Rev. Mol. Cell Biol.* **2008**, *9*, 112–124.

(8) Chiantia, S.; Ries, J.; Schwille, P. *Biochim. Biophys. Acta* **2009**, *1788*, 225–233.

(9) Eggeling, C.; Ringemann, C.; Medda, R.; Schwarzmann, G.; Sandhoff, K.; Polyakova, S.; Belov, V. N.; Hein, B.; von Middendorff, C.; Schonle, A.; Hell, S. W. *Nature* **2009**, *457*, 1159–1162.

(10) Machan, R.; Hof, M. *Biochim. Biophys. Acta* **2010**, *1798*, 1377–1391.

(11) Owen, J. S.; Bruckdorfer, K. R.; Day, R. C.; McIntyre, N. *J. Lipid Res.* **1982**, *23*, 124–132.

(12) Avdulov, N. A.; Chochina, S. V.; Igbavboa, U.; Ohare, E. O.; Schroeder, F.; Cleary, J. P.; Wood, W. G. *J. Neurochem.* **1997**, *68*, 2086–2091.

(13) Solans, R.; Motta, C.; Sola, R.; La Ville, A. E.; Lima, J.; Simeon, P.; Montella, N.; Armadans-Gil, L.; Fonollosa, V.; Vilardell, M. *Arthritis Rheum.* **2000**, *43*, 894–900.

(14) Chochina, S. V.; Avdulov, N. A.; Igbavboa, U.; Cleary, J. P.; O'Hare, E. O.; Wood, W. G. *J. Lipid Res.* **2001**, *42*, 1292–1297.

(15) Cazzola, R.; Rondanelli, M.; Russo-Volpe, S.; Ferrari, E.; Cestaro, B. *J. Lipid Res.* **2004**, *45*, 1846–1851.

(16) Sergent, O.; Pereira, M.; Belhomme, C.; Chevanne, M.; Huc, L.; Lagadic-Gossmann, D. *J. Pharmacol. Exp. Ther.* **2005**, *313*, 104–111.

(17) Spector, A. A.; Yorek, M. A. *J. Lipid Res.* **1985**, *26*, 1015–1035.

(18) Ladha, S.; Mackie, A. R.; Harvey, L. J.; Clark, D. C.; Lea, E. J. A.; Brullemans, M.; Duclohier, H. *Biophys. J.* **1996**, *71*, 1364–1373.

(19) Kahya, N.; Schwille, P. *J. Fluoresc.* **2006**, *16*, 671–678.

(20) Halliwell, B.; Chirico, S. *Am. J. Clin. Nutr.* **1993**, *57*, S715–S725.

(21) Porter, N. A.; Caldwell, S. E.; Mills, K. A. *Lipids* **1995**, *30*, 277–290.

(22) Niki, E.; Kawakami, A.; Yamamoto, Y.; Kamiya, Y. *Bull. Chem. Soc. Jpn.* **1985**, *58*, 1971–1975.

(23) Di Mascio, P.; Murphy, M. E.; Sies, H. *Am. J. Clin. Nutr.* **1991**, *53*, S194–S200.

(24) Wang, F.; Wang, T. H.; Lai, J. H.; Li, M.; Zou, C. G. *Biochem. Pharmacol.* **2006**, *71*, 799–805.

(25) Maruoka, N.; Murata, T.; Omata, N.; Takashima, Y.; Fujibayashi, Y.; Wada, Y. *J. Psychopharmacol.* **2008**, *22*, 119–127.

(26) Simons, K.; Ikonen, E. *Science* **2000**, *290*, 1721–1726.

(27) Saher, G.; Brugger, B.; Lappe-Siefke, C.; Mobius, W.; Tozawa, R.; Wehr, M. C.; Wieland, F.; Ishibashi, S.; Nave, K. A. *Nat. Neurosci.* **2005**, *8*, 468–475.

(28) Katsuno, M.; Adachi, H.; Sobue, G. *Nat. Med.* **2009**, *15*, 253–254.

(29) Lange, Y.; Swaisgood, M. H.; Ramos, B. V.; Steck, T. L. *J. Biol. Chem.* **1989**, *264*, 3786–3793.

(30) Echegoyen, S.; Oliva, E. B.; Sepulveda, J.; Diazzagoya, J. C.; Espinosagarcia, M. T.; Pardo, J. P.; Martinez, F. *Biochem. J.* **1993**, *289*, 703–708.

(31) Lange, Y.; Ramos, B. V. *J. Biol. Chem.* **1983**, *258*, 15130–15134.

(32) Magde, D.; Elson, E. L.; Webb, W., W. *Biopolymers* **1974**, *13*, 29–61.

(33) Chiantia, S.; Kahya, N.; Schwille, P. *Langmuir* **2007**, *23*, 7659–7665.

(34) Guo, L.; Har, J. Y.; Sankaran, J.; Hong, Y. M.; Kannan, B.; Wohland, T. *ChemPhysChem* **2008**, *9*, 721–728.

(35) Ghosh, S.; Adhikari, A.; Sen Niojumdar, S.; Bhattacharyya, K. *J. Phys. Chem. B* **2010**, *114*, 5736–5741.

(36) Xie, C. G.; Dinno, M. A.; Li, Y. Q. *Opt. Lett.* **2002**, *27*, 249–251.

(37) Chan, J. W.; Esposito, A. P.; Talley, C. E.; Hollars, C. W.; Lane, S. M.; Huser, T. *Anal. Chem.* **2004**, *76*, 599–603.

(38) Chang, W. T.; Lin, H. L.; Chen, H. C.; Wu, Y. M.; Chen, W. J.; Lee, Y. T.; Liau, I. *J. Raman Spectrosc.* **2009**, *40*, 1194–1199.

(39) Angelova, M. I.; Dimitrov, D. S. *Faraday Discuss.* **1986**, *81*, 303–311.

(40) Schwille, P.; Korlach, J.; Webb, W. W. *Cytometry* **1999**, *36*, 176–182.

(41) Garcia-Saez, A. J.; Schwille, P. *Methods* **2008**, *46*, 116–122.

(42) Chang, W. T.; Yang, Y. C.; Lu, H. H.; Li, I. L.; Liau, I. *J. Am. Chem. Soc.* **2010**, *132*, 1744–1745.

(43) Tejero, I.; Gonzalez-Lafont, A.; Lluch, J. M.; Eriksson, L. A. *J. Phys. Chem. B* **2007**, *111*, 5684–5693.

(44) Timmins, G. S.; dosSantos, R. E.; Whitwood, A. C.; Catalani, L. H.; Di Mascio, P.; Gilbert, B. C.; Bechara, E. J. H. *Chem. Res. Toxicol.* **1997**, *10*, 1090–1096.

(45) De Vico, L.; Liu, Y. J.; Krogh, J. W.; Lindh, R. *J. Phys. Chem. A* **2007**, *111*, 8013–8019.

(46) Nagasaka, R.; Okamoto, N.; Ushio, H. *Comp. Biochem. Physiol., Part C: Toxicol. Pharmacol.* **2004**, *139*, 259–266.

(47) Bendich, A.; Machlin, L. J.; Scandurra, O.; Burton, G. W.; Wayner, D. D. M. *Adv. Free Radical Biol. Med.* **1986**, *2*, 419–444.

(48) Xie, W. L.; Ji, J. M. *J. Food Biochem.* **2008**, *32*, 766–781.

(49) Pike, L. J. *J. Lipid Res.* **2003**, *44*, 655–667.

(50) Richter, C.; Gogvadze, V.; Laffranchi, R.; Schlapbach, R.; Schweizer, M.; Suter, M.; Walter, P.; Yaffee, M. *Biochim. Biophys. Acta* **1995**, *1271*, 67–74.

(51) Hoek, T. L. V.; Shao, Z. H.; Li, C. Q.; Schumacker, P. T.; Becker, L. B. *J. Mol. Cell. Cardiol.* **1997**, *29*, 2441–2450.